

# Localized electronic states of a terminated superlattice with a $\delta$ defect in the subsurface region

A. Kaczyński, R. Kucharczyk, and M. Stęślicka

*Institute of Experimental Physics, University of Wrocław, plac Maksa Borna 9, 50–204 Wrocław, Poland*

(Received 2 October 1998)

A Kronig-Penney-type model has been generalized to describe a semi-infinite GaAs/ $\text{Al}_x\text{Ga}_{1-x}\text{As}$  superlattice (SL), terminated by an  $\text{Al}_y\text{Ga}_{1-y}\text{As}$  substrate, and containing a single  $\delta$  defect in the subsurface region. Analytical expressions for the energy of localized states, appearing inside the minigaps, have been derived using a direct multimatching procedure within an envelope-function approximation. Numerical computations of the electronic structure have been performed for variable  $\delta$ -defect position with respect to the SL surface and different—modelistic as well as realistic—values of the  $\delta$ -function potential strength. Various SL surface conditions, corresponding to the terminating potential barrier higher, equal, and lower than the SL barriers, have been considered. The obtained results indicate that both the energy spectrum and space-charge distributions of localized states can be tailored by an appropriate choice of the SL surface conditions (i.e., parameters of the SL/substrate interface) and the parameters (the strength as well as the position) of the inserted  $\delta$  defect. [S0163-1829(99)08307-1]

## I. INTRODUCTION

In the past decade, an otherwise extensive field of research of electronic properties of superlattices (SL's) has been enriched by considering the effects of various SL potential perturbations. In particular, a SL termination by a substrate or a cap layer has been taken into account and the consequent occurrence of SL surface states (i.e., the states lying within energetic minigaps and confined to the SL/substrate interface) has been predicted theoretically<sup>1–4</sup> and shown experimentally.<sup>5–8</sup> In a series of papers (see, for example, Refs. 9–12 and references therein), surface-state properties have been thoroughly studied and some peculiar features of SL surface states, making them interesting for specific device applications, have been noticed.<sup>13,14</sup>

On the other hand, SL structures with spatially localized defects, such as fluctuations in SL layer thicknesses or the so-called  $\delta$  defects (i.e., intentionally inserted impurities confined to a single monolayer), have been investigated for a variety of purposes (see, for example, Refs. 15–29 and references therein). Such perturbations of an otherwise perfect SL substantially modify its optical and transport characteristics<sup>15,17–20,26,29</sup> and, in particular, may give rise to the appearance—inside energy minigaps—of discrete states localized at the defect site.<sup>16,24,25,27</sup>

In reality, the impurities are introduced in terminated SL's, hence both the above-mentioned perturbations of the SL potential are simultaneously present. If the defect is located close enough to the SL surface, a strong interaction between the impurity-induced and surface states should occur, similarly as it happens for nearly-free-electron metals.<sup>30</sup> The aim of the present paper is to explore this effect in SL's by investigating the energy spectrum as well as space-charge distributions of all localized states.

## II. MODEL

To describe a semi-infinite SL with a  $\delta$  defect in the subsurface region, a generalized Kronig-Penney-type model is

applied. The corresponding potential profile is schematically plotted in Fig. 1. SL well and barrier layers are of thicknesses  $a$  and  $b$  and effective-masses  $m_a$  and  $m_b$ , respectively, while  $V_b$  stands for the SL potential barrier height. SL is terminated by a step potential  $V_s$  representing the substrate with an effective-mass  $m_s$ .

The additional impurity is represented by a  $\delta$ -function potential of strength  $p$ . On the one hand, this kind of potential reflects in the simplest way the fact that the inserted defect is spatially strongly localized, while, on the other hand, enables an analytical handling of the problem.<sup>18</sup> The parameter  $p$  is considered to be either positive (as in Fig. 1) or negative, which corresponds to the repulsive or attractive interaction, respectively. The impurity can be located at an arbitrary distance  $q$  from the SL surface.

## III. METHOD OF CALCULATION

In the present paper, we restrict ourselves to investigate the appearance and properties of electronic states occurring within the energy minigaps and being confined to the subsurface region of the SL. The calculations are performed

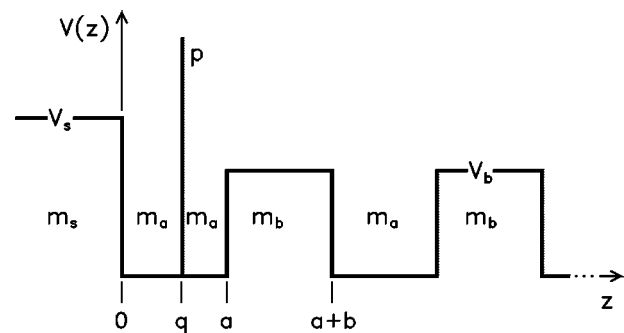


FIG. 1. Potential profile of the structure under consideration. Semi-infinite SL is described by a generalized Kronig-Penney-type model, terminated by a potential step representing a substrate. The defect, located in the subsurface SL region, is represented by a  $\delta$ -function potential. For notation, see the text.

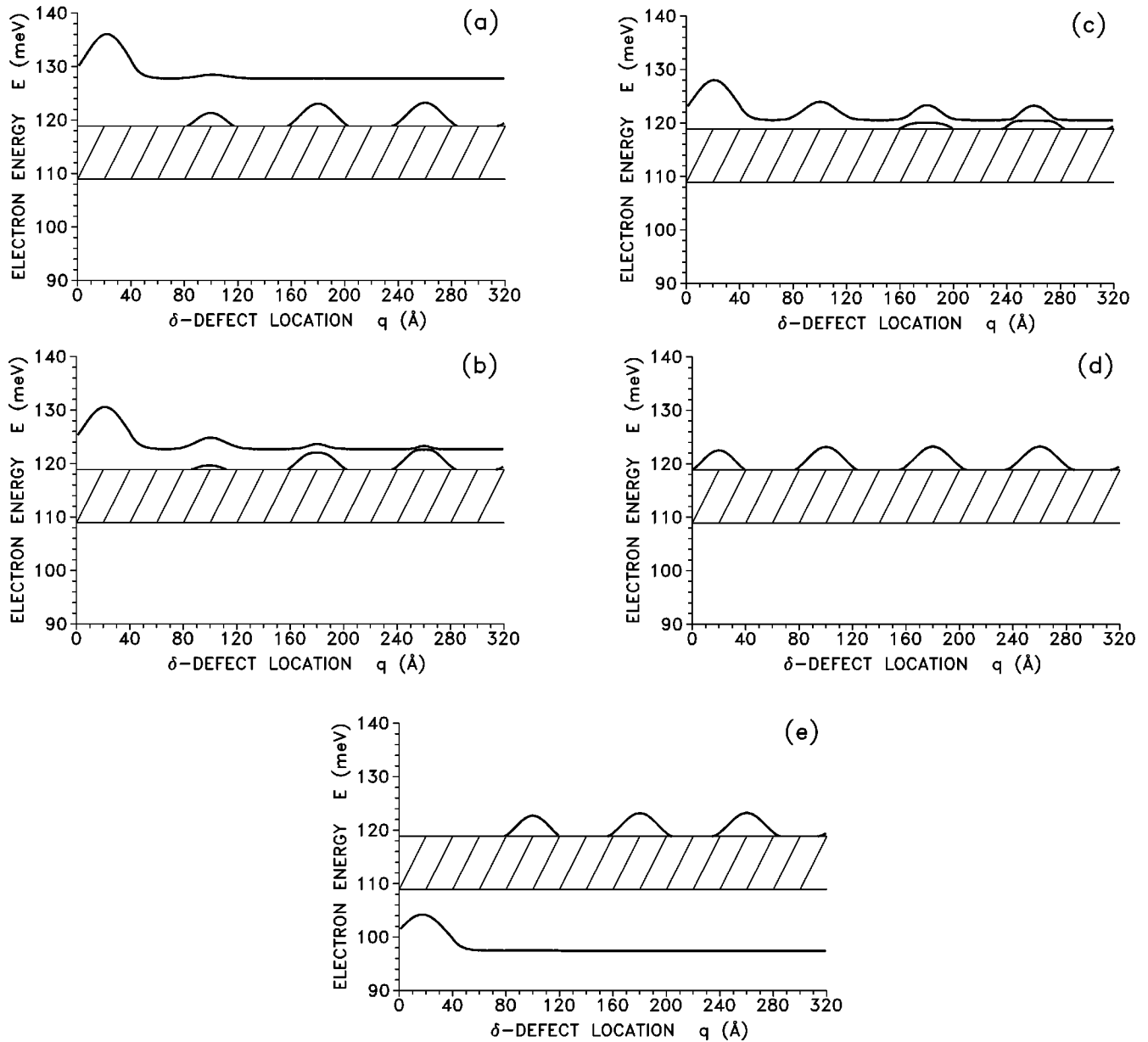


FIG. 2. Influence of the  $\delta$ -defect location relative to the SL surface  $q$  on the energy spectrum of localized states (solid lines) appearing in the vicinity of the lowest miniband (shaded area) for a semi-infinite GaAs/Al<sub>0.4</sub>Ga<sub>0.6</sub>As SL with  $a=b=40$  Å, terminated by a substrate with (a)  $y=1$ , (b)  $y=0.65$ , (c)  $y=0.55$ , (d)  $y=0.4$ , and (e)  $y=0.2$ . The  $\delta$ -potential strength is fixed at  $p=+0.02$ . Zero of the energy axis corresponds to the bottom of GaAs conduction band, i.e., the bottom of SL wells in Fig. 1.

using the direct multimatching procedure within an envelope-function approximation.

As a first step to obtain the energy expression for localized states, we construct the wave functions  $\psi_r(z)$  and  $\psi_l(z)$ , appropriate for regions to the right and to the left of the  $\delta$  defect, respectively. The wave function  $\psi_r(z)$  is a linear combination of sine and cosine (or: hyperbolic sine and hyperbolic cosine), whose coefficients are determined by matching, at the nearest right-hand-side well/barrier interface, to the appropriate SL Bloch wave function. The latter has a required decaying character into the SL (for  $z \rightarrow \infty$ ), since the Bloch wave number is complex within the minigaps (cf. Refs. 4 and 11). The wave function  $\psi_l(z)$  is again a combination of trigonometric (hyperbolic) functions, but this time the coefficients are obtained from a multiple matching at the left-hand-side well/barrier interfaces, with the final

matching, at the SL surface, to the exponential function decaying into the substrate (for  $z \rightarrow -\infty$ ).

The next step is to match  $\psi_l(z)$  and  $\psi_r(z)$  at  $z=q$  (the position of the  $\delta$  defect), using the following continuity conditions

$$\psi_l(q) = \psi_r(q) \quad (1a)$$

and

$$\psi'_r(q) - \psi'_l(q) = 2m^* p \psi_l(q), \quad (1b)$$

where  $m^*$  equals to  $m_a$  or  $m_b$  depending on whether the  $\delta$  defect is located inside the well or barrier layer. From the requirement that nontrivial solutions of Eq. (1) exist, the energy equation for localized states can be obtained.

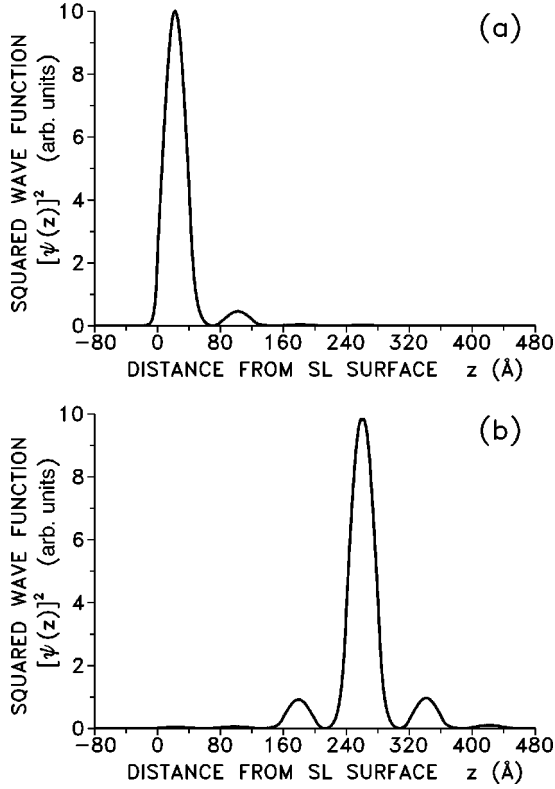


FIG. 3. Squared wave functions of localized states corresponding to  $p = +0.02$  and  $q = 260$  Å (i.e.,  $\delta$  defect located in the middle of the fourth SL well) for  $y = 1$  [cf. Fig. 2(a)]: (a) higher-energy state with  $E = 127.7$  meV; (b) lower-energy state with  $E = 123.2$  meV.

To be more specific, for  $\delta$  defect located within the outermost SL well ( $0 < q < a$ ), this expression takes the following form:

$$\begin{aligned} & \frac{2m_a p}{k_a} [\sin(k_a q) + G \cos(k_a q)] \{S(E) \sin(k_a q) \\ & + K \cos[k_a(a - q)] \sinh(k_b b) \\ & + \sin[k_a(a - q)] \cosh(k_b b)\} \\ & + K [\cos(k_a a) - G \sin(k_a a)] \sinh(k_b b) \\ & + [\sin(k_a a) + G \cos(k_a a)] \cosh(k_b b) - GS(E) = 0, \end{aligned} \quad (2)$$

where  $K = (k_a m_b) / (k_b m_a)$ ,  $G = (k_a m_s) / (k_s m_a)$ ,  $k_a = \sqrt{2m_a E}$ ,  $k_b = \sqrt{2m_b(V_b - E)}$ , and  $k_s = \sqrt{2m_s(V_s - E)}$ , while

$$S(E) = B(E) \pm \sqrt{B^2(E) - 1}, \quad (3)$$

with

$$\begin{aligned} B(E) &= \cos(k_a a) \cosh(k_b b) \\ &+ \frac{1}{2} (K^{-1} - K) \sin(k_a a) \sinh(k_b b) \end{aligned} \quad (4)$$

being the right-hand side of a standard SL bulk dispersion relation (see, for example, Ref. 16). In Eq. (3), minus and plus correspond to even and odd minigaps, respectively.<sup>4,11</sup>

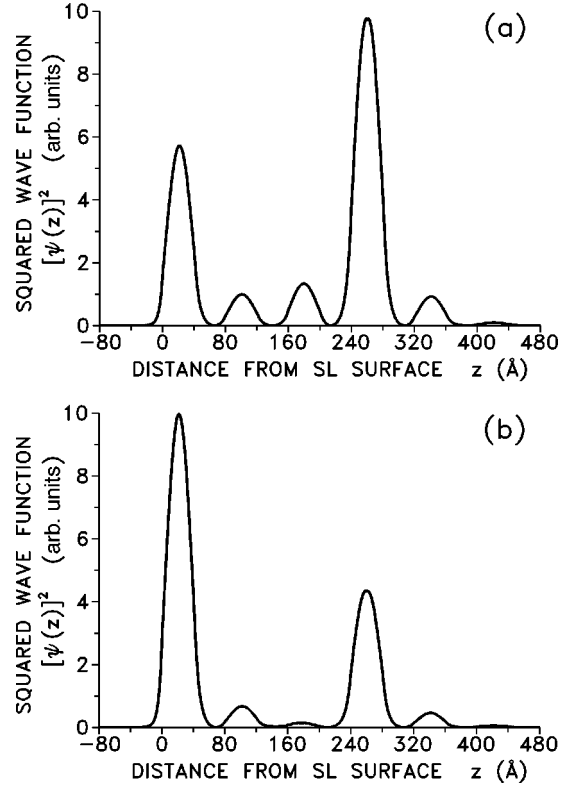


FIG. 4. The same as in Fig. 3, but for  $y = 0.65$  [cf. Fig. 2(b)]: (a) higher-energy state with  $E = 123.3$  meV; (b) lower-energy state with  $E = 122.9$  meV.

For the  $\delta$  defect inserted in successive SL layers, the energy equations for localized states have also been derived in a similar way, however, they can no longer be expressed in such a concise form.

#### IV. RESULTS AND DISCUSSION

Numerical calculations have been performed for  $\delta$ -defected GaAs/Al<sub>x</sub>Ga<sub>1-x</sub>As SL's terminated by an Al<sub>y</sub>Ga<sub>1-y</sub>As substrate. To reduce the number of variables, the widths of SL layers and the concentration of Al in SL barriers have been fixed at  $a = b = 40$  Å and  $x = 0.4$ , which leads to  $V_b = 377.6$  meV,  $m_a = 0.067$ , and  $m_b = 0.1102$ . This set of bulk SL parameters results in a rather narrow first miniband ranging from 108.9 to 118.8 meV (note that all energies are relative to the bottom of GaAs conduction band, i.e., the bottom of SL wells in Fig. 1).

To examine the interaction between the impurity-induced and surface states, the  $\delta$ -defect position relative to the SL surface  $q$  has been varied within a few subsurface SL periods, while the  $\delta$ -potential strength  $p$  was kept constant. To follow the most characteristic features of localized states, two values of the parameter  $p$  have been assumed, namely,  $p = 0.02$ , which is a rather modelistic value, and  $p = 0.2$ , which corresponds to deep-center defects in semiconductors, with ionization energies reported in Ref. 31.

For the case of  $p = 0.02$ , the energy spectrum of localized states appearing in the vicinity of the lowest miniband is shown in Fig. 2 for different concentrations  $y$  of Al in the substrate, simulating various surface conditions with the ter-

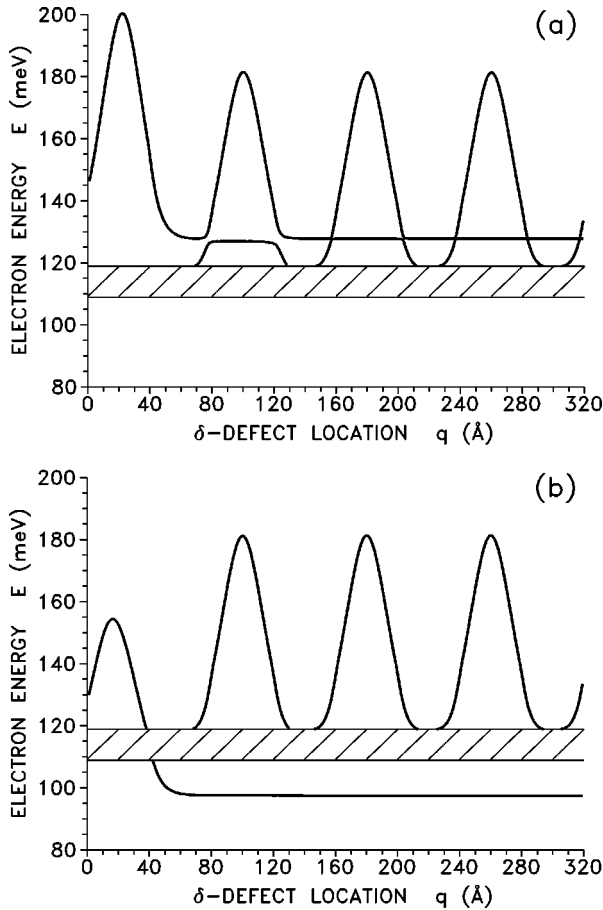


FIG. 5. The same as in Fig. 2, but for the  $\delta$ -potential strength  $p = +0.2$  and surface conditions corresponding to (a)  $y = 1$  and (b)  $y = 0.2$ .

minating potential step higher, equal, and lower than the SL barriers.

As can be seen in Fig. 2(a), for  $y = 1$  the distance  $q \geq 3(a + b) = 240 \text{ \AA}$  is already large enough for the  $\delta$  defect and the SL surface not to influence each other. Therefore, the upper curve does not depend on  $q$  and represents the energy of a surface state of an impurity-free SL (i.e., surface state appearing in the model of Fig. 1 with  $p = 0$ ). On the other hand, the lower energy curve exhibits the  $q$ -dependence coinciding with that for a single  $\delta$  defect inserted in an infinite SL. Wave functions corresponding to both states are presented in Fig. 3 for  $q = 260 \text{ \AA}$  (i.e., for the  $\delta$  defect located in the middle of the fourth SL well) and they clearly do not overlap. When the  $\delta$  defect is located closer to the SL surface, the respective wave functions start to overlap, but the character of the spectrum does not really change to about  $q \approx (a + b) = 80 \text{ \AA}$ . For the  $\delta$  defect lying within the outermost SL period, the impurity-induced state merges into the miniband, while the wave function of the remaining state has the same form as that of Fig. 3(a).

When the difference  $(y - x)$  becomes smaller, the upper curve moves towards lower energies, and thus, for large enough  $q$ , intersects the lower curve, as is illustrated in Figs. 2(b) and 2(c) for  $y = 0.65$  and  $y = 0.55$ , respectively. The presented plots indicate that any intersection of curves exhibits a typical anticrossing feature. For  $q$  close to the crossing points, the interaction of both states is strong, which results

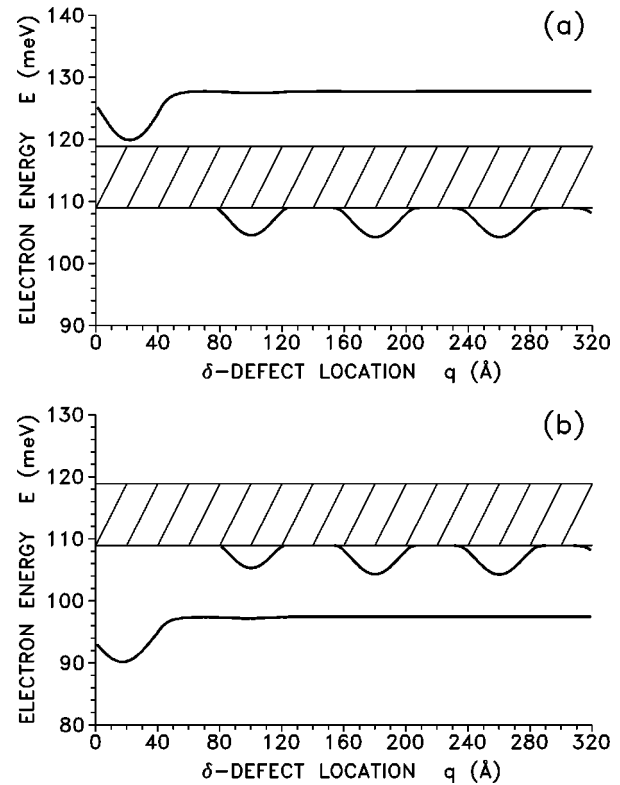


FIG. 6. The same as in Fig. 2, but for the  $\delta$ -potential strength  $p = -0.02$  and surface conditions corresponding to (a)  $y = 1$  and (b)  $y = 0.2$ .

in their ‘‘mixed’’ character, as follows from the shape of the corresponding wave functions, possessing two distinct maxima at the surface and the defect site (cf. Fig. 4 for  $y = 0.65$  and  $q = 260 \text{ \AA}$ ). For the  $\delta$  defect approaching the SL surface, the wave function of the remaining localized state takes again the form of that of Fig. 3(a). Consequently, by varying the  $\delta$ -defect position relative to the SL surface, the space-charge distributions associated with particular states can be manipulated. It should be noticed that when the difference between the surface and SL potential barriers decreases, but is still large enough to generate a surface state (in our case,  $y \geq 0.5$ ), the lower-energy state appears for larger and larger values of  $q$  [cf. Figs. 2(a)–2(c)].

For  $y$  close to  $x$  and, in particular, for  $y = x$ , surface states never occur in a terminated impurity-free SL (see, for example, Ref. 11). Consequently, the spectrum of the SL with a  $\delta$  defect consists of one state only [cf. Fig. 2(d) for  $y = 0.4$ ], whose wave function resembles that of Fig. 3(b).

When  $y$  is smaller than  $x$  ( $y \leq 0.35$ ), a surface state appears below the miniband, while the impurity-induced state still exists above the miniband [cf. Fig. 2(e) for  $y = 0.2$ ]. As expected, the two localized states almost do not interact with each other and their wave functions coincide with those shown in Fig. 3.

Consider now the case of  $p = 0.2$ , with the most representative results presented in Fig. 5. As can be seen, the  $q$ -dependence of the impurity-induced-state energy is now much more pronounced, which leads to the intersection of both energy curves already for  $y = 1$  [cf. Fig. 5(a)]. For  $y = 0.2$ , the energy spectrum is similar to that of Fig. 2(e) except for the maximum of the lower curve occurring now,

within the outermost SL well, above the miniband [cf. Fig. 5(b)].

Finally, the computations have also been performed for negative values of the  $\delta$ -potential strength  $p$  (i.e., for an attractive impurity). It has been found that the energy spectra of localized states for  $p < 0$  exhibit, in principle, the same features as those for  $p > 0$ . For example, the spectrum for  $p = -0.02$  and  $y = 1$  ( $y = 0.2$ ) is, in fact, a mirror reflection, with respect to the miniband center, of that for  $p = +0.02$  and  $y = 0.2$  ( $y = 1$ ) [cf. Fig. 6(a) vs Fig. 2(e) and Fig. 6(b) vs Fig. 2(a)].

## V. SUMMARY

A Kronig-Penney-type model has been generalized to describe a semi-infinite GaAs/Al<sub>x</sub>Ga<sub>1-x</sub>As SL, terminated by an Al<sub>y</sub>Ga<sub>1-y</sub>As substrate, and containing a single  $\delta$  defect in the subsurface region. Analytical expressions for the energy of localized states, appearing inside the minigaps, have been derived using a direct multimatching procedure within an envelope-function approximation. Numerical computations of the electronic structure in a vicinity of the lowest miniband have been performed for variable  $\delta$ -defect position with respect to the SL surface and different—modelistic as well as realistic—values of the  $\delta$ -function potential strength. Various SL surface conditions have also been considered, with the terminating potential barrier higher, equal, and lower than the SL barriers.

The obtained results indicate that introduction of a  $\delta$  defect into the subsurface region provides a useful means for modifying the electronic properties of a terminated SL. To

be more specific, the energy spectrum of localized states as well as their space-charge distributions (the latter follows from the analysis of the corresponding wave functions) critically depend on both the SL surface conditions (i.e., parameters of the SL/substrate interface) and the parameters (the strength as well as the position) of the inserted  $\delta$  defect. In general, two localized states—one due to the SL termination (surface state), while the other generated by the presence of a  $\delta$  defect (impurity-induced state)—can appear; in particular, both of them may occur in the same (higher or lower) minigap, or the spectrum may consist of one localized state in each of the considered minigaps. The energy spectrum may also be reduced to only one, impurity-induced state. In each case, the energy position of all localized states can be arbitrarily shifted within the minigaps.

Finally, it has been shown that the localized states may exhibit a “pure” or “mixed” character, depending on whether the corresponding wave function has one pronounced maximum, either at the SL surface (“pure” surface state) or at the  $\delta$ -defect site (“pure” impurity-induced state), or two distinct maxima at both the SL surface and the  $\delta$  defect (“mixed” state). Thus, the space-charge distributions associated with localized states can be manipulated. We believe that these particular properties of the considered  $\delta$ -doped SL’s might be essential with respect to their specific device applications.

## ACKNOWLEDGMENTS

Support by the University of Wrocław within Grant No. 2016/W/IFD/98 is gratefully acknowledged.

- <sup>1</sup>V. Milanović, *Physica B* **121**, 181 (1983).
- <sup>2</sup>P. Masri, L. Dobrzynski, B. Djafari-Rouhani, and J. O. A. Idioudi, *Surf. Sci.* **166**, 301 (1986).
- <sup>3</sup>J. Zhang and S. E. Ulloa, *Phys. Rev. B* **38**, 2063 (1988).
- <sup>4</sup>M. Stęślicka, R. Kucharczyk, and M. L. Glasser, *Phys. Rev. B* **42**, 1458 (1990).
- <sup>5</sup>H. Ohno, E. E. Mendez, J. A. Brum, J. M. Hong, F. Agulló-Rueda, L. L. Chang, and L. Esaki, *Phys. Rev. Lett.* **64**, 2555 (1990).
- <sup>6</sup>F. Agulló-Rueda, E. E. Mendez, H. Ohno, and J. M. Hong, *Phys. Rev. B* **42**, 1470 (1990).
- <sup>7</sup>H. Ohno, E. E. Mendez, A. Alexandrou, and J. M. Hong, *Surf. Sci.* **267**, 161 (1992).
- <sup>8</sup>T. Miller and T.-C. Chiang, *Phys. Rev. Lett.* **68**, 3339 (1992).
- <sup>9</sup>P. Masri, *Surf. Sci. Rep.* **19**, 1 (1993).
- <sup>10</sup>J. Arriaga, F. García-Moliner, and V. R. Velasco, *Prog. Surf. Sci.* **42**, 271 (1993).
- <sup>11</sup>M. Stęślicka, *Prog. Surf. Sci.* **50**, 65 (1995).
- <sup>12</sup>E.-H. El Boudouti, B. Djafari-Rouhani, A. Akjouj, L. Dobrzynski, R. Kucharczyk, and M. Stęślicka, *Phys. Rev. B* **56**, 9603 (1997).
- <sup>13</sup>F. Y. Huang, *Appl. Phys. Lett.* **57**, 1669 (1990).
- <sup>14</sup>J. Zhang, S. E. Ulloa, and W. L. Schaich, *Phys. Rev. B* **43**, 9865 (1991).
- <sup>15</sup>P. Voisin, G. Bastard, C. E. T. Gonçalves da Silva, M. Voos, L. L. Chang, and L. Esaki, *Solid State Commun.* **39**, 79 (1981).
- <sup>16</sup>G. Bastard, *Phys. Rev. B* **25**, 7584 (1982).
- <sup>17</sup>F. Capasso, K. Mohammed, and A. Y. Cho, *Phys. Rev. Lett.* **57**, 2303 (1986).
- <sup>18</sup>F. Beltram and F. Capasso, *Phys. Rev. B* **38**, 3580 (1988).
- <sup>19</sup>K. Ploog, M. Hauser, and A. Fisher, *Appl. Phys. A: Solids Surf.* **45**, 233 (1988).
- <sup>20</sup>E. F. Schubert, *Surf. Sci.* **228**, 240 (1990).
- <sup>21</sup>M. He and B.-Y. Gu, *Phys. Rev. B* **41**, 2906 (1990).
- <sup>22</sup>L. N. Pandey, T. F. George, M. L. Rustgi, and D. Sahu, *J. Appl. Phys.* **68**, 5724 (1990).
- <sup>23</sup>G. Ihm, S. K. Noh, J. I. Lee, J.-S. Hwang, and T. W. Kim, *Phys. Rev. B* **44**, 6266 (1991).
- <sup>24</sup>F. Capasso, C. Sirtori, J. Faist, D. L. Sivco, S.-N. G. Chu, and A. Y. Cho, *Nature (London)* **358**, 565 (1992).
- <sup>25</sup>R. A. Suris and P. Lavallard, *Phys. Rev. B* **50**, 8875 (1994).
- <sup>26</sup>B. Jonsson, A. G. Larsson, O. Sjölund, S. Wang, T. G. Andersson, and J. Maserjian, *IEEE J. Quantum Electron.* **QE-30**, 63 (1994).
- <sup>27</sup>K. A. Mäder, L.-W. Wang, and A. Zunger, *J. Appl. Phys.* **78**, 6639 (1995).
- <sup>28</sup>H. Xu and G. Chen, *Phys. Status Solidi B* **191**, K17 (1995).
- <sup>29</sup>G. Schwarz, F. Prengel, E. Schöll, J. Kastrop, H. T. Grahn, and R. Hey, *Appl. Phys. Lett.* **69**, 626 (1996).
- <sup>30</sup>I. Bartoš and P. Jaroš, *Prog. Surf. Sci.* **42**, 35 (1993).
- <sup>31</sup>G. Lucovsky, *Solid State Commun.* **3**, 299 (1965).